J. Civil Eng. Mater.App. 2025 (December); 9(4): 177-189

Journal of Civil Engineering and Materials Application
Journal home page: http://jcema.com

Received: 13 October 2025 • Revised: 20 November 2025 • Accepted: 14 December 2025

Research

doi: 10.22034/jcema.2025.560653.1186

Investigation of the Effect of FRP Fibers on the Seismic Retrofit of Reinforced Concrete Flat-Slab Frames with Openings under Cyclic Loading

Seyed Ali Mousavi Davoudi

Department of Engineering and Civil Engineering, Mazandaran National University of Skills, Sari, Iran.

*Correspondence should be addressed to Seyed Ali Mousavi Davoudi, Department of Engineering and Civil Engineering, Mazandaran National University of Skills, Sari, Iran. Email: ali_mousavii@yahoo.com

ABSTRACT

Flat slab systems are susceptible to brittle punching shear failure at slab–column connections, which may trigger progressive collapse. This study aims to evaluate and compare the effectiveness of fiber-reinforced polymer (FRP) strengthening with conventional concrete and steel jacketing techniques in enhancing the punching shear performance of reinforced concrete flat slabs. A five-story reinforced concrete building with a flat slab system was designed using ETABS and subsequently modeled in ABAQUS for detailed finite element analysis. Three retrofit scenarios, including FRP strengthening, concrete jacketing, and steel jacketing, were numerically investigated and compared in terms of load-carrying capacity, deformation response, and failure behavior at slab–column connections. The results indicate that FRP strengthening significantly improves punching shear resistance and stiffness while providing higher energy absorption capacity compared to the other techniques. In contrast, concrete and steel jacketing increase structural weight and exhibit less efficient performance enhancement. Overall, FRP strengthening demonstrated superior efficiency in improving structural safety and mitigating punching shear failure in flat slab systems, highlighting its practicality as an effective retrofit solution.

Keywords: Cyclic loading, Reinforced concrete frame, Retrofit, Flat slab, Finite element analysis

1. INTRODUCTION

Flat slabs are generally designed to resist only vertical loads, while lateral load–resisting systems are responsible for carrying seismic lateral forces. Nevertheless, significant shear forces develop at the slab–column connections. During the 1985 Mexico City earthquake, 91 flat-slab structures collapsed and 44 others experienced severe damage due to punching shear failures [1]. In Iran, a large number of reinforced concrete buildings of both low and high rise utilize flat slab systems, with or without shear walls. As previously discussed, these structures require vulnerability assessment and retrofitting due to their susceptibility to damage. Past investigations and case studies, considering the existing structural conditions, have shown that one of the most effective seismic strengthening strategies for buildings that have available exterior space is the

use of externally installed lateral-resisting elements. This strengthening approach involves minimal demolition, causes the least disruption to the building's functionality, and allows continued occupancy during construction [2,3].

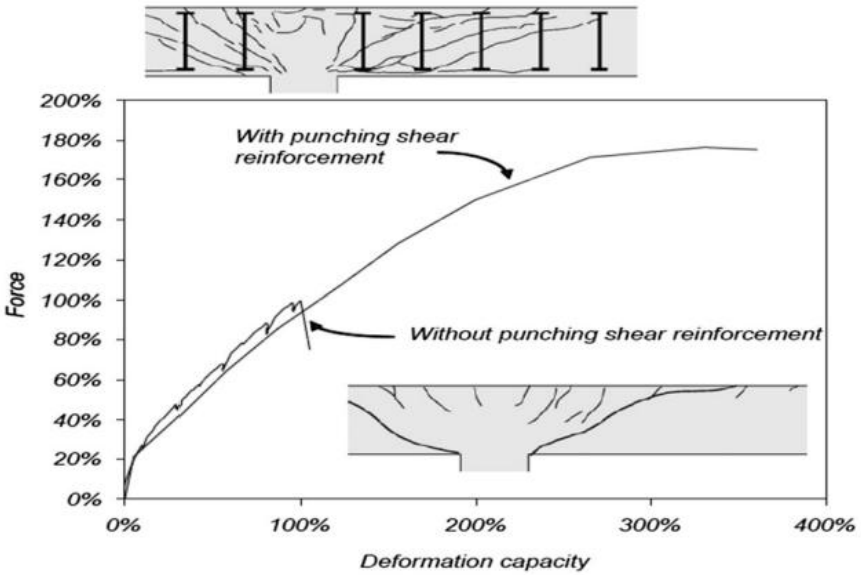

Figure 1. View of flat slab strengthening and structural components [2]

It has also been observed that the use of shear walls in both longitudinal and transverse directions for interior panels results in the lowest retrofit cost. Moreover, the use of external bracing elements combined with internal shear walls, or the installation of internal bracing systems alone, generally entails higher costs compared to the shear wall option. The incorporation of shear walls significantly enhances the strength, stiffness, ductility, and reliability of the structure, thereby improving its seismic behavior and reducing deformations and damage to other concrete components [4].

Seismic retrofitting is a modern branch of civil engineering that has been widely recognized in industrialized countries for several decades. In recent years, due to the considerable damage caused by past earthquakes, this field has gained increasing importance in Iran as well [4]. Given that Iran lies along the Alpine–Himalayan seismic belt, numerous earthquakes occur annually in various regions of the country. The Iranian Seismic Code (Standard 2800) classifies most densely populated cities as high or very high seismic hazard zones [5].

One of the most effective approaches to reducing earthquake-induced damage is the retrofitting of existing buildings. The urgency of this issue becomes even more pronounced considering the presence of deteriorated urban fabrics in seismic-prone regions, widespread construction without adherence to proper standards, and the use of outdated design codes in previous decades. The absence of beams in flat slab systems simplifies construction, accelerates the building process, increases the clear story height, and reduces the overall height of the structure. However, the susceptibility of slab–column connections to brittle punching shear failure makes these systems vulnerable to progressive collapse. Such failures can occur suddenly, without prior warning signs, due to the inherently brittle nature of punching shear, which is an undesirable characteristic in seismic design [6-9].

Beheshti and Motaghi (2017), in a study on a deficient six-story reinforced concrete building, concluded that one of the key aspects of seismic retrofitting is providing a basis for comparing different design and retrofit alternatives using concepts such as collapse performance. They retrofitted a weak RC building using two different methods steel bracing and friction dampers and developed numerical models for each. By selecting 15 ground–motion records, they performed Incremental Dynamic Analysis (IDA) on all three models. Their results indicated that both retrofit methods reduced the probability of structural collapse at both IO (Immediate Occupancy) and CP (Collapse Prevention) performance levels. However, when incorporating the seismic hazard curve of the region taking into account the structural stiffness characteristics different outcomes were obtained [10].

Benisi and Bayrak (2003) introduced a new method to enhance the punching shear capacity of slabs. They placed FRP steel plates perpendicular to the slab surface around the column and perpendicular to the flexural reinforcement, functioning as shear reinforcement. Their observations showed that the potential punching shear failure plane shifted away from the column vicinity, and the punching capacity increased by approximately 55 percent. In recent years, the strengthening of reinforced concrete structures using FRP composites has received significant attention; however, the strengthening of two-way slabs, particularly with the aim of improving punching shear resistance, has not been extensively investigated. At Razi University, a study was conducted on strengthening flat slabs using FRP and steel plates to enhance their punching shear capacity. In this method, fiber-reinforced polymer elements were placed as closed stirrup-like assemblies within the slab depth. All tested specimens exhibited increases in ultimate strength, displacement capacity, absorbed energy, and ductility [11]. Despite the widespread use of FRP for strengthening reinforced concrete members, the seismic behavior of reinforced concrete flat slab frame systems, particularly at the critical slab–column connections under cyclic loading, has not been sufficiently investigated. Moreover, direct and quantitative comparisons between FRP strengthening and conventional concrete and steel jacketing techniques remain limited in the existing literature. Therefore, this study is necessary to identify the most efficient retrofit method for improving the seismic safety of flat slab systems.

2. METHODOLOGY

The investigated model in this study is a five-story reinforced concrete structure with a flat slab system, which will be modeled, analyzed, and designed using ETABS software. For the evaluation of various retrofitting scenarios, the finite element software ABAQUS will be employed. The model specifications and influential parameters are presented in Table (1), while the structural plan dimensions and details are illustrated in Figure (2).

Table 1. Specifications and influential parameters of the case study specimen

Sample Name	Number of Stories	Influential Parameter
A-1	3 story	**Unstrengthened**
A-2		**FRP Strengthened**
A-3		**Concrete Jacketing Strengthened**
A-4		**Steel Jacket Strengthened**

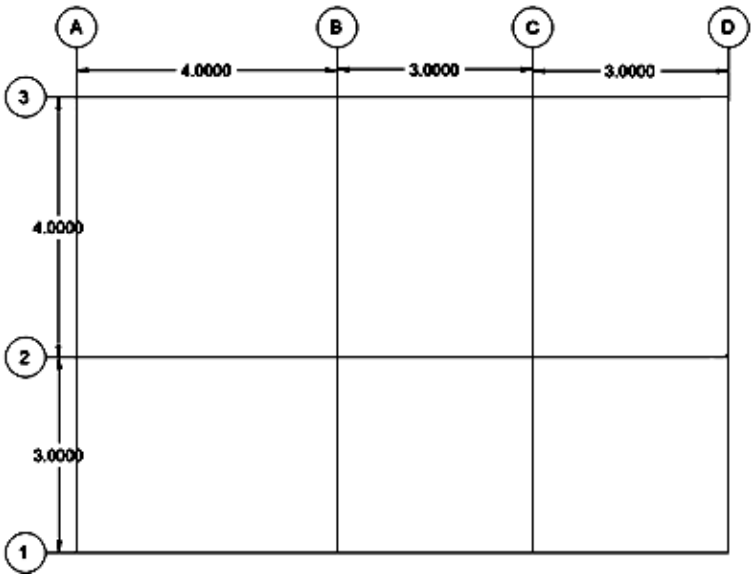

Figure 2. Plan of the Studied Structure

2.1. Mechanical Properties of Concrete

To define concrete in the finite element software ABAQUS, a material behavior model called the Concrete Damaged Plasticity (CDP) model is available. This model provides a general capability for simulating the behavior of concrete or any other quasi-brittle material. [3] It models the inelastic behavior of concrete by combining isotropic damage concepts within the elastic range with compressive plasticity in the plastic range. [7]

In this study, the reinforced concrete flat slab system was numerically modeled using ABAQUS. Concrete was modeled with 3D solid elements (C3D8R) and the Concrete Damaged Plasticity model to capture cracking and crushing behavior. Reinforcement bars were represented by T3D2 truss elements with an elastic–plastic constitutive law, and the interaction between concrete and steel was defined using the Embedded Region approach. FRP sheets were modeled with shell elements (S4R) and assumed fully bonded to the concrete surface. This modeling approach provides a suitable balance between computational accuracy and efficiency.

In this study, the concrete used in the investigated model has a compressive strength of 25 MPa. The behavior of the concrete follows both elastic and plastic properties. Figure (3) illustrates the stress–strain curve of the concrete employed in the modeling of the specimens in this research.

Table 2. Mechanical Properties of the Concrete

Concrete Compressive Strength (mpa)	Density (kg/m^2)
25	2500

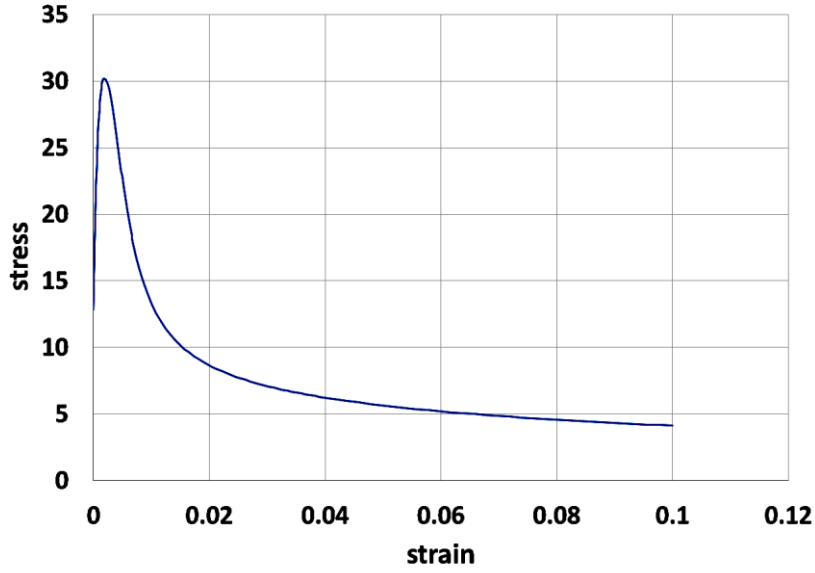

Figure 3. Stress–Strain Curve of Concrete Used in Specimen Modeling [7]

2.2. Mechanical Properties of Reinforcement Bars

In this study, the reinforcement bars are made of S400 steel. To simplify the definition of the nonlinear mechanical behavior of steel reinforcement, the stress–strain curve of the steel is assumed to be bilinear. Therefore, it is sufficient to define two slopes as the initial and secondary elastic moduli along with the yield stress [8,9]. The properties of the S400 steel used in this modeling are presented in Tables (3 to 5).

Table 3. Mechanical Properties of Reinforcement Bars for Specimen B

Rebar Type	Poisson's Ratio	Density (kg/m^3)	Elastic Modulus (MPa)
S400	0.3	7850	$2.05E10^5$

Table 4. Linear Isotropic Mechanical Properties of Steel

Poisson's ratio	Elastic modulus (MPa)
0.3	$2.05E10^5$

Table 5. Bilinear Isotropic Mechanical Properties of Steel

Stress (MPa)	Strain
465	**0**
600	**0.12**

For the validation of the Abaqus model, the experimental study conducted by Yang Sung et al. (2014) was utilized [5]. After modeling the laboratory specimen in Abaqus and comparing the load–displacement curves, a very small difference of approximately 2.4% was observed. Figures (5 and 6) present the laboratory specimen and its corresponding load–displacement curve.

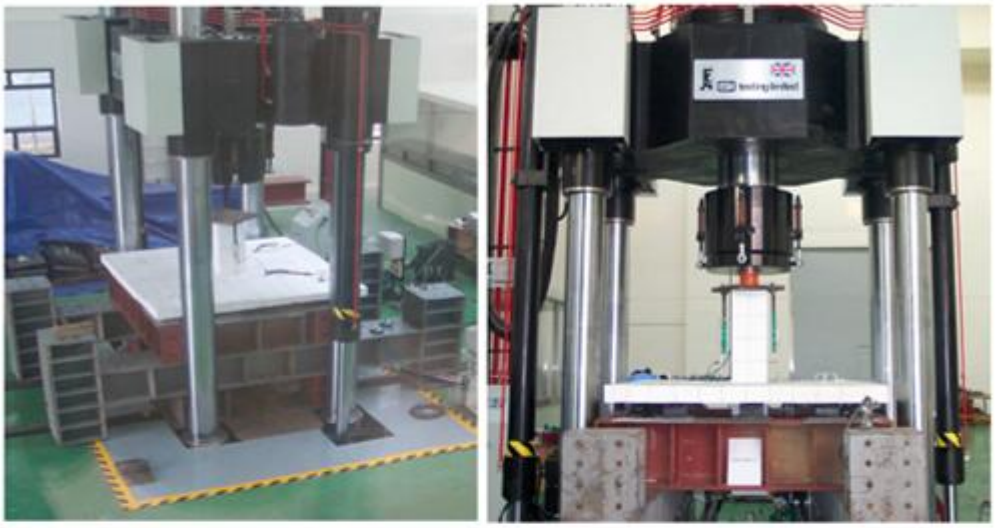

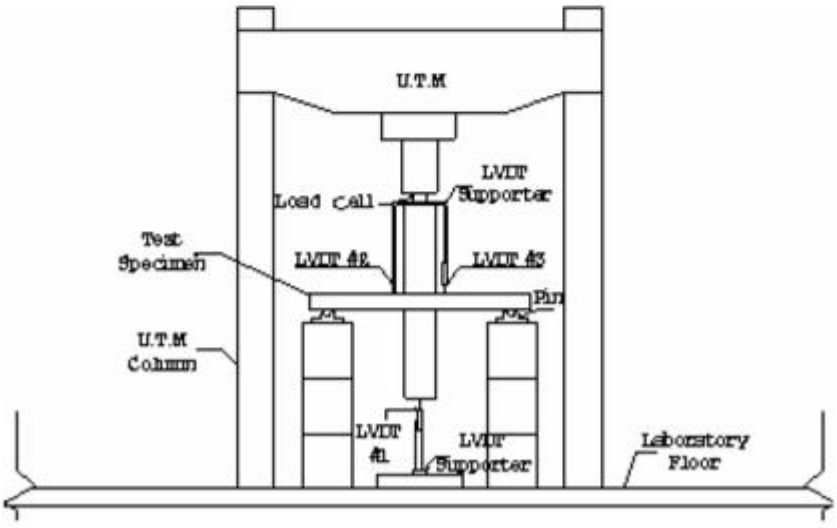

Figure 4. Geometry of the Validated Laboratory Specimen by Yang Sung et al. [5]

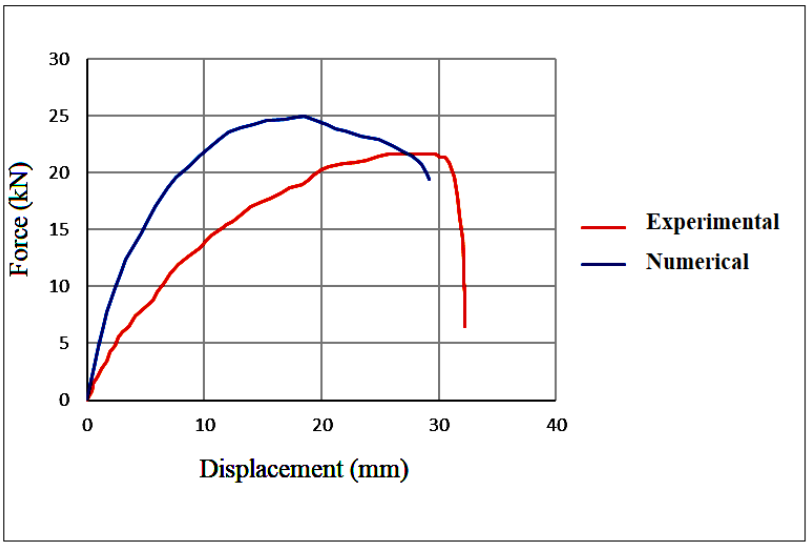

Figure 5. Validation Curve of Yang Sung et al. Laboratory Specimen and Numerical Analysis [5]

For modeling the designed specimens, the finite element software ABAQUS was employed. Solid elements were used to model the concrete, while Wire elements were utilized for the steel reinforcement bars. During the material definition stage in ABAQUS, both linear and nonlinear behavior of the materials was considered. [8,9] The mechanical properties of S400 steel reinforcement and concrete with a compressive strength of 25 MPa were applied. To connect all rigid parts, the Tie constraint was used, and the Contact constraint (surface-to-surface) was defined for all surfaces in contact with each other. The geometric components created for the study specimen can be observed in Figure (6).

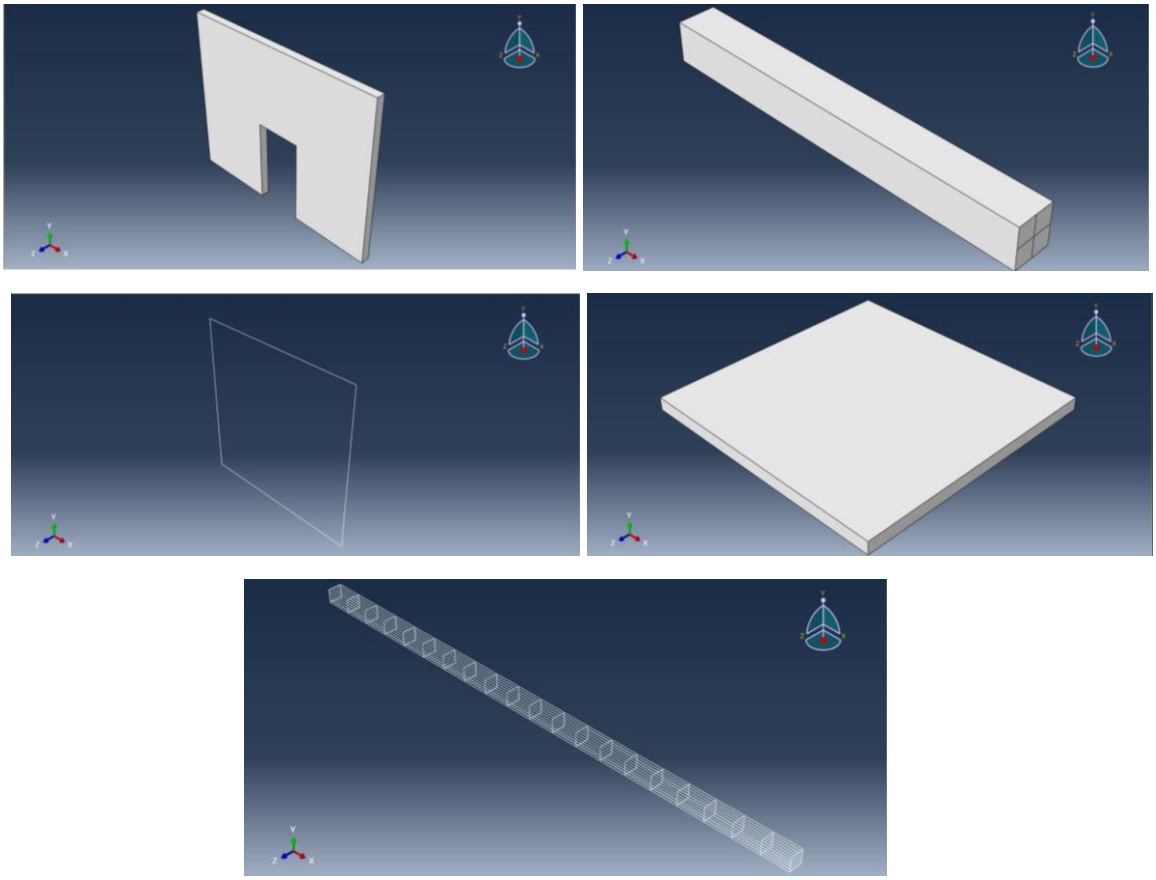

Figure 6. View of the Created Model Components in the ABAQUS Graphical Environment

Solid elements were used to model the concrete components, while Wire elements were employed for the steel reinforcement bars. [12,13]. The modulus of elasticity of the steel was 199 GPa, and the concrete used in this modeling was confined concrete with a compressive strength of 25 MPa.

After defining the material properties of both concrete and steel, the materials were assigned to the respective parts. Once the materials were assigned, the corresponding parts turned green. Figure 7 illustrates the assignment of materials to the modeled specimen [8,14].

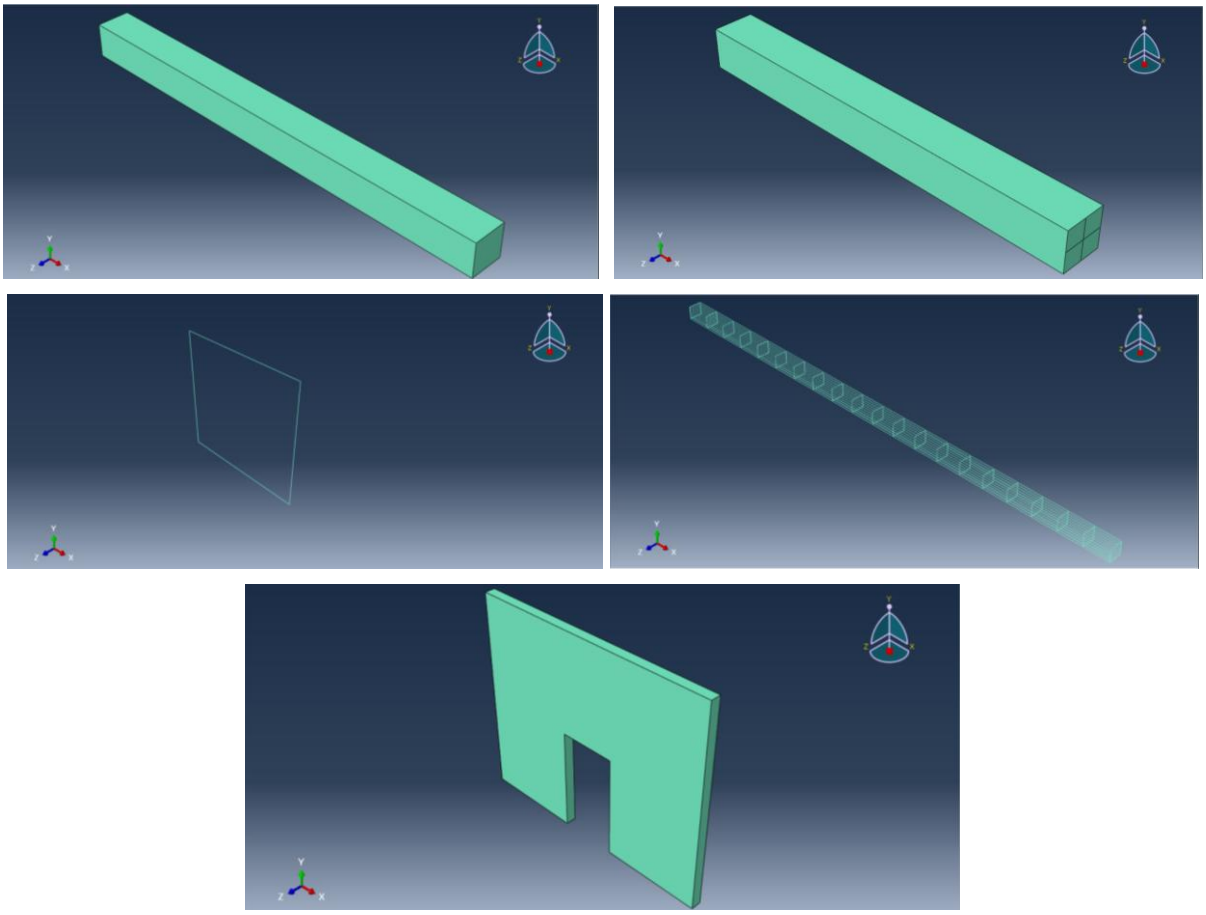

Figure 7. View of Created Parts in the ABAQUS Material Assignment Module

The Assembly module is used for assembling the model. In this section, all individual parts of the model are created and assembled. After completing the assembly, the final configuration of the model can be observed in the Assembly graphical environment.

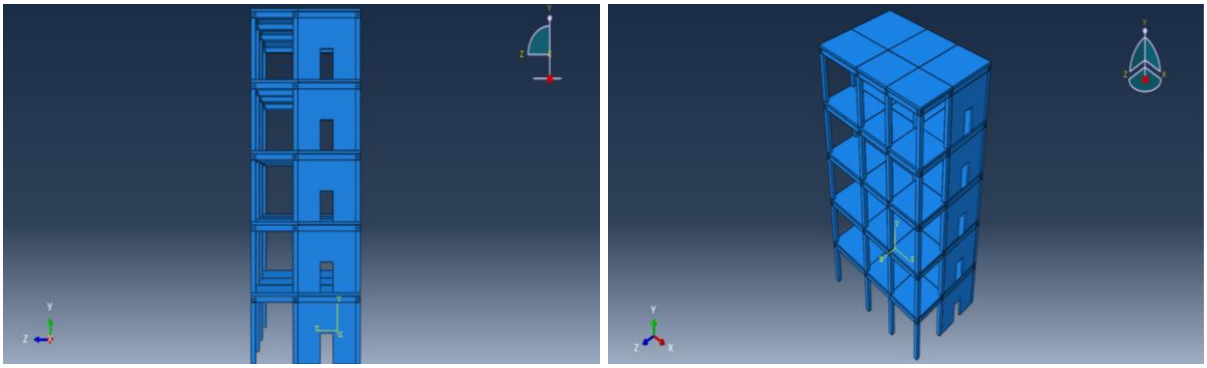

Figure 8. Model View in the ABAQUS Assembly Module Graphical Environment

To apply dead and live vertical loads, the load type in the Load module of ABAQUS was selected as gravitational. For the application of cyclic loading, the load–time history shown in Figure (9) was defined for all specimens.

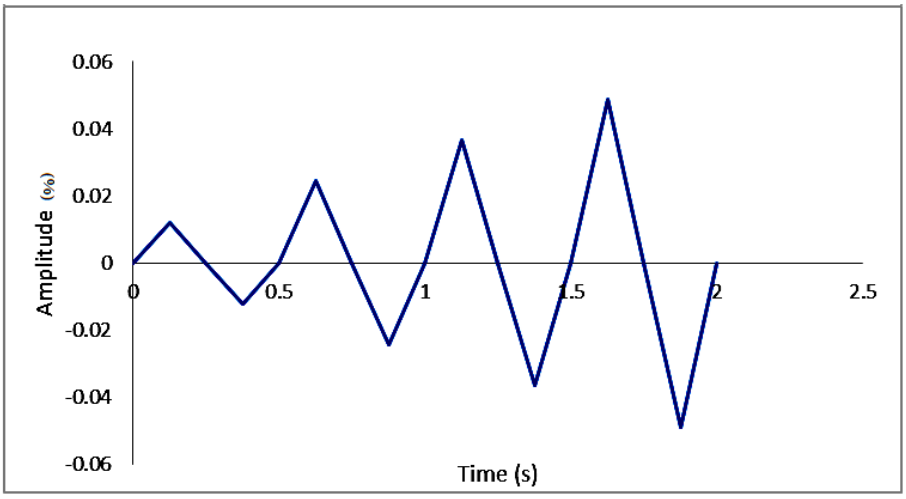

Figure 9. Cyclic loading diagram

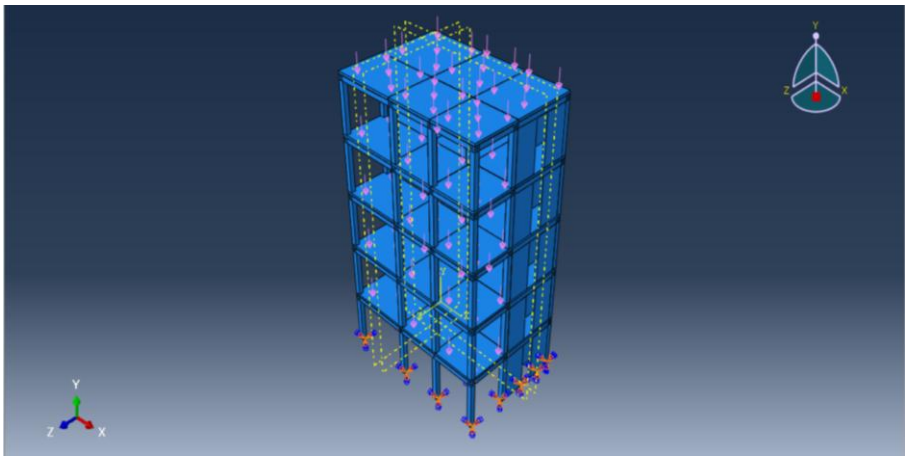

Figure 10. Load Application in the ABAQUS Load Module Graphical Environment

In the Mesh module, the finite element meshing of the model was performed. A mesh size of 50 mm was assigned. Figure (11) illustrates the meshing configuration.

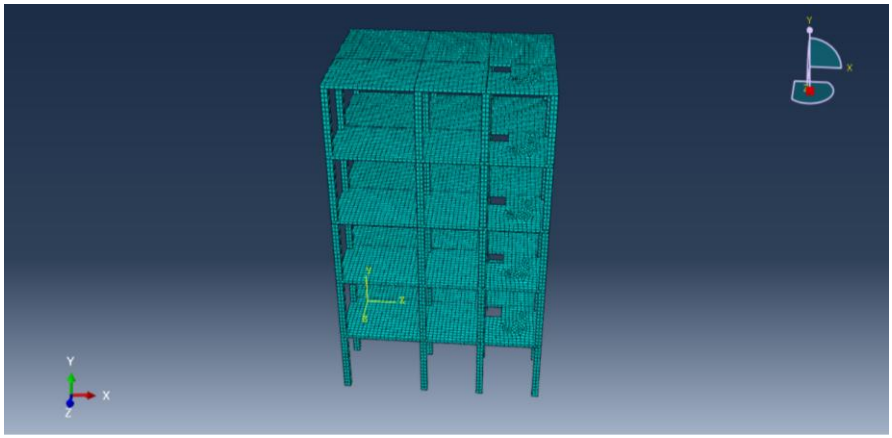

Figure 11. Meshed Model in the ABAQUS Graphical Environment

After performing the analysis, the results of the cyclic loading can be visualized using the visualization module of ABAQUS. Figures (12 to 15) present the contour plots of the analyzed contour of the total displacement (U-magnitude) of the specimen, indicating that the combined displacements are greater at the ends and corners of the slab under impulsive loads.

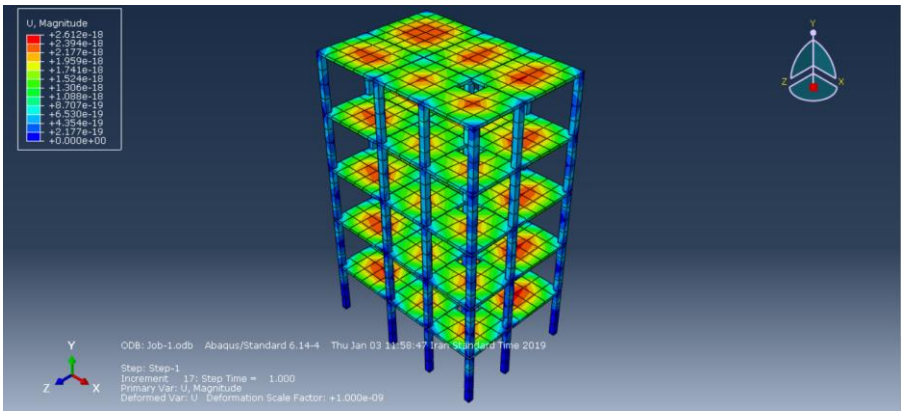

Figure 12. Contour Plot of Displacement Distribution for the Unstrengthened Model

After performing the analysis under impulsive loading in ABAQUS, the displacement contour for specimen A-1 is presented in Figure (13). By examining and analyzing the stress contour, it can be observed that the maximum displacement occurs at the mid-span regions of the slab in the unstrengthened model A-1.

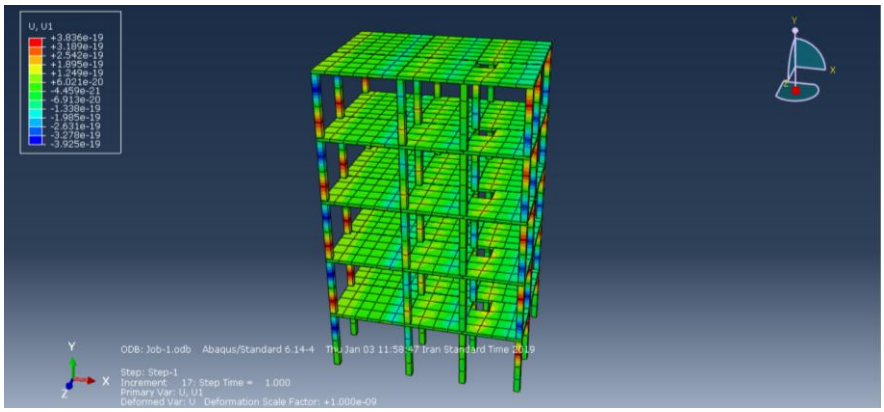

Figure 13. Contour Plot of Displacement Distribution for the Model Strengthened with Steel Jacketing

By examining the displacement contour of specimen A-2, which was strengthened with steel plates, it was observed that the steel plate reinforcement improved the slab performance compared to the unstrengthened case.

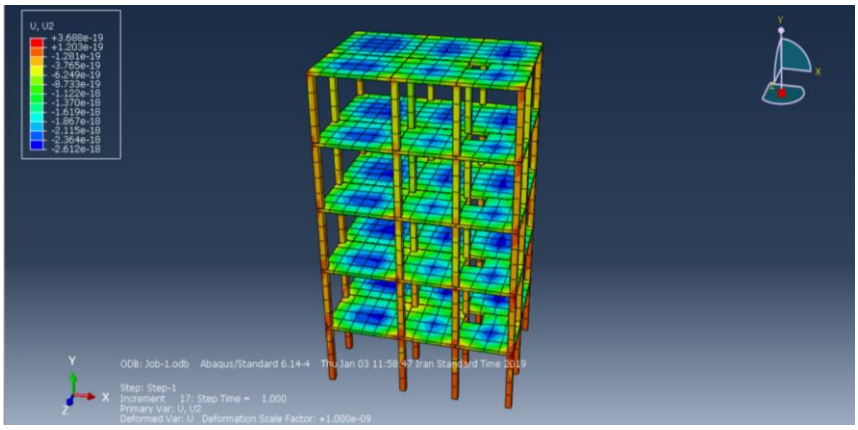

Figure 14. Displacement Distribution of the Model Strengthened with Concrete Jacketing

By examining Figure (12), which shows the displacement contour for specimen A-3, strengthened with a concrete jacketing, it is observed that the concrete jacketing performs better than the steel jacketing, resulting in improved structural behavior. This improvement is reflected in the redistribution of displacements.

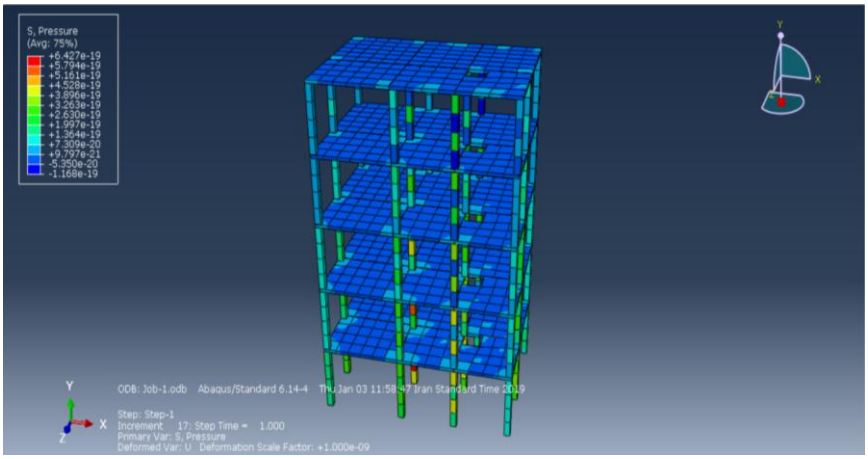

Figure 15. Displacement Distribution of the Model Strengthened with FRP Sheets

3. RESULTS AND DISCUSSION

After modeling the analytical specimens in ABAQUS, the hysteresis curves of the structure were extracted from the software's visualization module. Figures (16 to 19) present the hysteresis diagrams for all four specimens. As shown in Figure (16), the unstrengthened specimen reached a maximum load capacity of 142.62 kN at a displacement of 2.61 cm.

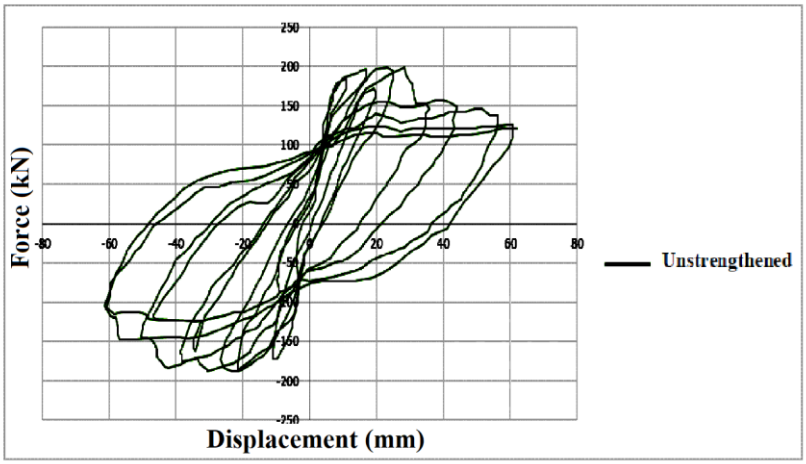

Figure 16. Hysteresis Curve of the Unstrengthened Model

In Figure (17), which presents the hysteresis curve of the specimen strengthened with a steel jacketing, it is shown that the specimen strengthened with FRP sheets exhibits an increased load capacity, reaching a maximum of 591.34 kN at a displacement of 42.61 cm.

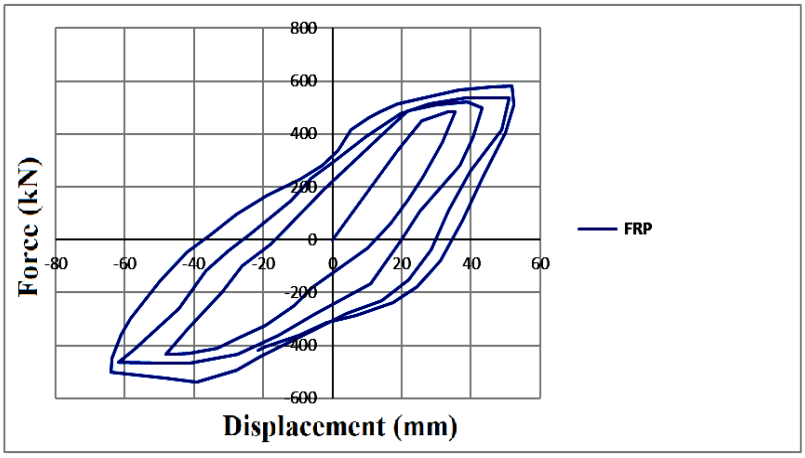

Figure 17. Hysteresis Curve of the Model Strengthened with FRP Sheets

In Figure (18), which shows the hysteresis curve of the specimen strengthened with concrete jacketing, it is evident that the load capacity of the specimen increases compared to the unstrengthened case, reaching a maximum of 489.51 kN at a displacement of 51.31 cm.

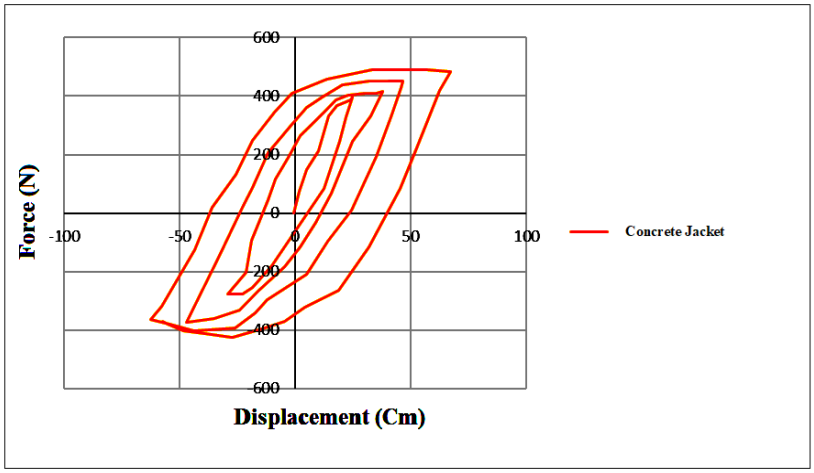

Figure 18. Hysteresis Curve of the Model Strengthened with Concrete Jacketing

In Figure (19), which presents the hysteresis curve of the specimen strengthened with steel jacketing, it is observed that the load capacity of the specimen increases compared to the unstrengthened case, reaching a maximum of 231.71 kN at a displacement of 68.85 cm.

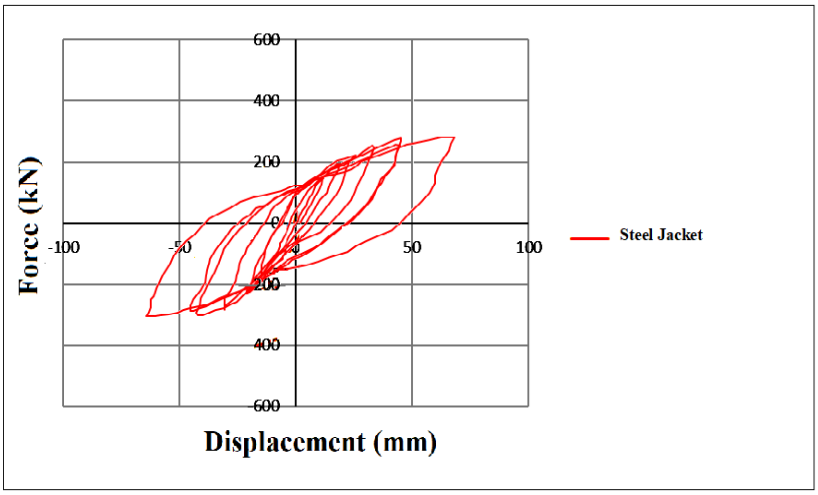

Figure 19. Hysteresis Curve of the Model Strengthened with Steel Jacketing

Figure (20) presents a comparative hysteresis diagram of the studied specimens: unstrengthened, strengthened with steel plates, strengthened with concrete jacketing, and strengthened with FRP sheets. By comparing the specimens, it is evident that the specimen strengthened with FRP sheets exhibits the highest and most favorable mechanical performance. Following the FRP-strengthened specimen, the specimen strengthened with concrete jacketing demonstrates the next best behavior. Finally, the specimen strengthened with steel jacketing shows the weakest mechanical performance among the studied cases.

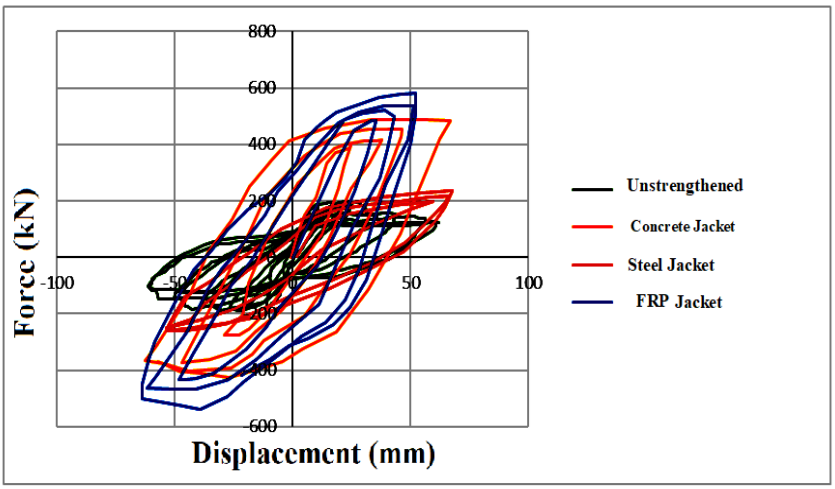

Figure 20. Comparative Hysteresis Diagram of the Analytical Specimens

4. CONCLUSION

Based on the comparison of the unstrengthened and strengthened models, it was observed that the average load-bearing capacity of the strengthened section is 23.85% higher than that of the unstrengthened section. Similarly, the average stiffness of the strengthened section is 18.2% higher than that of the unstrengthened model, and the average ductility of the strengthened section is 16.34% higher than that of the unstrengthened model.

Considering the hysteresis curves of the models strengthened with steel jacketing and concrete jacketing, it was observed that the load capacity of the concrete-jacketed model is 12.8% higher than that of the steel-jacketed model. The stiffness of the concrete-jacketed model is 10.75% higher, and its ductility is 11.75% higher than those of the steel-jacketed model.

By comparing the hysteresis curves of the model strengthened with FRP sheets to the concrete-jacketed model, it was found that the load capacity of the FRP-strengthened model is 16.28% higher than that of the concrete-jacketed model. The stiffness of the FRP-strengthened model is 35.16% higher, and its ductility is 72.14% higher than those of the concrete-jacketed model.

FUNDING/SUPPORT
Not mentioned by Authors.

ACKNOWLEDGMENT
Not mentioned by Authors.

AUTHORS CONTRIBUTION
This work was carried out in collaboration among all authors.

CONFLICT OF INTEREST
The author (s) declared no potential conflicts of interests with respect to the authorship and/or publication of this paper.

5. REFERENCES

[1] Dehghan K, Kazeroonian SA. Investigating the effect of size and location of openings on the stiffness and flexibility of hollow concrete slabs (Cobiax). In: Proceedings of the 4th Scientific Research Congress on New Horizons in Civil Engineering, Architecture, Culture, and Urban Management; 2016; Tehran, Iran. Available from. [View at Publisher]

[2] Deputy of Technical Affairs and Standards Development. Iranian Concrete Code (ABA) – Part 2. 2nd ed. Publication No. 120. Danesh Nama Monthly. Nos. 170–171 (Tir–Mordad). Organization for Planning and Budget; n.d. [View at Publisher]

[3] Davoudi SM, Naghipour M. The effect of slenderness ratio on modification of compressive strength of AISC code for composite columns (CFT) T-shaped with numerical (FEM) and experimental analysis. Results Mater. 2021. [View at Google Scholar]; [View at Publisher]

[4] Wang Z. Understanding seismic hazard and risk assessments: an example in the New Madrid seismic zone of the central United States. In: Proceedings of the 8th U.S. National Conference on Earthquake Engineering; 2006 Apr 18–22; San Francisco, CA, USA. Paper No. 416. [View at Google Scholar]; [View at Publisher]

[5] Committee for Revision of the Iranian Seismic Design Code. Iranian code of practice for seismic resistant design of buildings (Standard No. 2800–84). 3rd ed. Publication No. Z–253. 6th printing. Building and Housing Research Center; 2005. p.125–135. [View at Publisher]

[6] Cho YS, Seo CJ, Kang ES. A study of flat plate slab–column connections with shear plate in tall concrete building using experimental and numerical analysis. In: Proceedings of the CTBUH 2004 Seoul Conference; 2004; Seoul, South Korea. Paper No. 1704. Council on Tall Buildings and Urban Habitat. [View at Google Scholar]; [View at Publisher]

[7] Mousavi DSA, Naghipour M. Studying the buckling behavior of composite columns (CFST) by cyclic loading. J Civ Eng Mater Appl. 2019;3(4):203-213. [View at Google Scholar]; [View at Publisher]

[8] Mousavi DS, Khalilipasha MH. A Study on the Structural Effects of Bagasse Sugar Cane Stem In Structural Concrete Mixture in Sulfate and Chloride Environments. [View at Google Scholar]; [View at Publisher]

[9] Mousavi Davoudi SA, Naghipour M. Presentation of critical buckling load correction factor of AISC code on L-shaped composite columns by numerical and experimental analysis. 2020;20:1682–1702. [View at Google Scholar]; [View at Publisher]

[10] Beheshti Aval B, Motaghi L. Effect of regional seismic hazard on the selection of retrofitting methods for defective reinforced concrete frames. Amirkabir J Civ Eng. 2017;49(3). [View at Google Scholar]; [View at Publisher]

[11] Binici B, Bayrak O. Punching shear strengthening of reinforced concrete flat plates using carbon fiber reinforced polymers. J Struct Eng (ASCE). 2003;129(9):1173–1182. [View at Google Scholar]; [View at Publisher]

[12] Mousavi Davoudi S, Neghipour M. A comparison of modal analysis of Ritz vector mode (Ritze) and Eagan vector (Eigen) based on nonlinear time history (NTH) dynamic analysis. J Struct Eng. 2020;16(4):21–32. [View at Publisher]

[13] Mousavi Davoudi S, Neghipour M. Investigation of the effective factors for eliminating the defect in the CFT columns with an asymmetric L-shaped columns by the finite element analysis. J Struct Eng. 2019;16(3):19–30. [View at Publisher]

[14] Mousavi Davoudi S, Neghipour M. Study of the behavior of composite steel columns filled with short (non-slender) concrete with (L)-shaped geometric cross section under numerical sensitivity analysis (FEM) with axial compression loading. J Struct Eng. 2019;15(4):37–50. [View at Publisher]